Geophys. J. Int. (2004) **156,** 575–583 doi: 10.1111/j.1365-246X.2004.02161.x

Local pattern of stress field and seismogenic sources in the Pergola–Melandro basin and the Agri valley (Southern Italy)

Luigi Cucci, Silvia Pondrelli, Alberto Frepoli, Maria Teresa Mariucci and Marco Moro
Istituto Nazionale di Geofisica e Vulcanologia, Rome, Italy. E-mail: cucci@ingv.it

Accepted 2003 October 17. Received 2003 October 17; in original form 2002 July 8

SUMMARY

Our study area is a *ca* 50 km long section of the central-southern Apennines tectonic belt that includes the Pergola–Melandro basin (PM) and the Agri valley (AV). This region is located between the areas affected by the 1980 $Ms = 6.9$ Irpinia and the 1857 $M = 7.0$ val d'Agri earthquakes and is characterized by rare historical events and very low and sparse background seismicity. In this study we provide new seismological and geophysical information to identify the characteristics of the seismotectonics in the area as the prevailing faulting mechanism and the fit of local to regional stress field. These data concern focal mechanisms from waveform modelling and *P*-wave polarities, analyses of borehole breakouts and detailed investigation of two seismic sequences. All the data cover a significantly broad range of magnitudes and depths and suggest that no important local variation in stress orientation seems to affect this area, which shows a NE–SW direction of extension consistent with that regionally observed in southern Italy. Such local homogeneity in the stress field pattern is peculiar to the study area; the variations of orientation and/or type of stress observed in the northern Apennines, or less than only 100 km toward the northwest within the same tectonic belt, are absent here. Furthermore, there is a suggestion for a northeastward sense of dip of the seismogenic faults in the region, an interesting constraint to the characterization of seismic sources.

Key words: faulting, seismicity, seismotectonics, southern Italy, stress distribution.

INTRODUCTION

Almost one century after the first intuitions of Omori (1909) about the distribution of the largest historical earthquakes in Italy, and following the first formulation of the central-southern Apennines seismogenic belt as a synthetic model of the seismogenesis in most of the Italian Peninsula (Valensise *et al.* 1993), several contributions have been provided to associate the large number of major earthquakes of the historical record to the small number of observable causative faults along the belt. These efforts led to the publication of a series of inventories and compilations of tectonic features such as active faults (Galadini *et al.* 2000), capable faults (Michetti *et al.* 2000) and seismogenic sources (Valensise & Pantosti 2001). Furthermore, regions of the Apennines where the lack of large seismicity was only due to the scarce historical record were given the appropriate seismogenic potential as in the Marsica, central Italy (Pantosti *et al.* 1996) and Pollino, southern Italy (Michetti *et al.* 1997; Cinti *et al.* 1997, 2002).

A closer look at the tectonic belt reveals evidence that parts of it have not experienced large historical earthquakes and are bounded on either or both sides by rupture zones of recent major earthquakes. Examples include the Mugello area along the northern Apennines, the Città di Castello zone in central Italy, and the region south of the 1980 Irpinia $Ms = 6.9$ earthquake in the southern Apennines. Such areas may be the most likely places for the occurrence of a large magnitude earthquake in the medium term.

Our study area is located in southern Italy between the Irpinia region to the north and the Calabria–Lucania border to the south (Fig. 1). This *ca* 1000 km^2 vast region is rather peculiar as it includes the Pergola–Melandro basin (PM), to the north, and the Agri Valley (AV), to the southeast, showing different seismotectonic interpretations. Uncertainties in the location of the seismogenic sources along these depressions are evident (Fig. 1): Michetti *et al.* (2000) suggest a southwest facing normal fault on the eastern side of the AV and do not recognize any sources along the PM basin; Galadini *et al.* (2000) suppose a northeast dipping normal fault along the PM and state the difficulty to recognize which is the main faulted side of the AV. Finally, Valensise & Pantosti (2001) envision similar northeast verging normal faults with different degrees of reliability along the two basins.

In the study area, the Catalogue of Strong Italian Earthquakes (Boschi *et al.* 2000) reports only two large historical earthquakes (Fig. 1): in 1857 in the central AV ($M = 7$) and in 1561 west of the PM ($M = 6.5$). Other significant events occurred in 1694 ($M = 6.9$), close to the Irpinia epicenter and in 1836 ($M = 6.3$), south of the AV. The plot of the 1981–2000 record of modern seismicity (Fig. 1) shows dense clusters of earthquakes related to the four main seismic sequences that occurred in the recent period, namely the

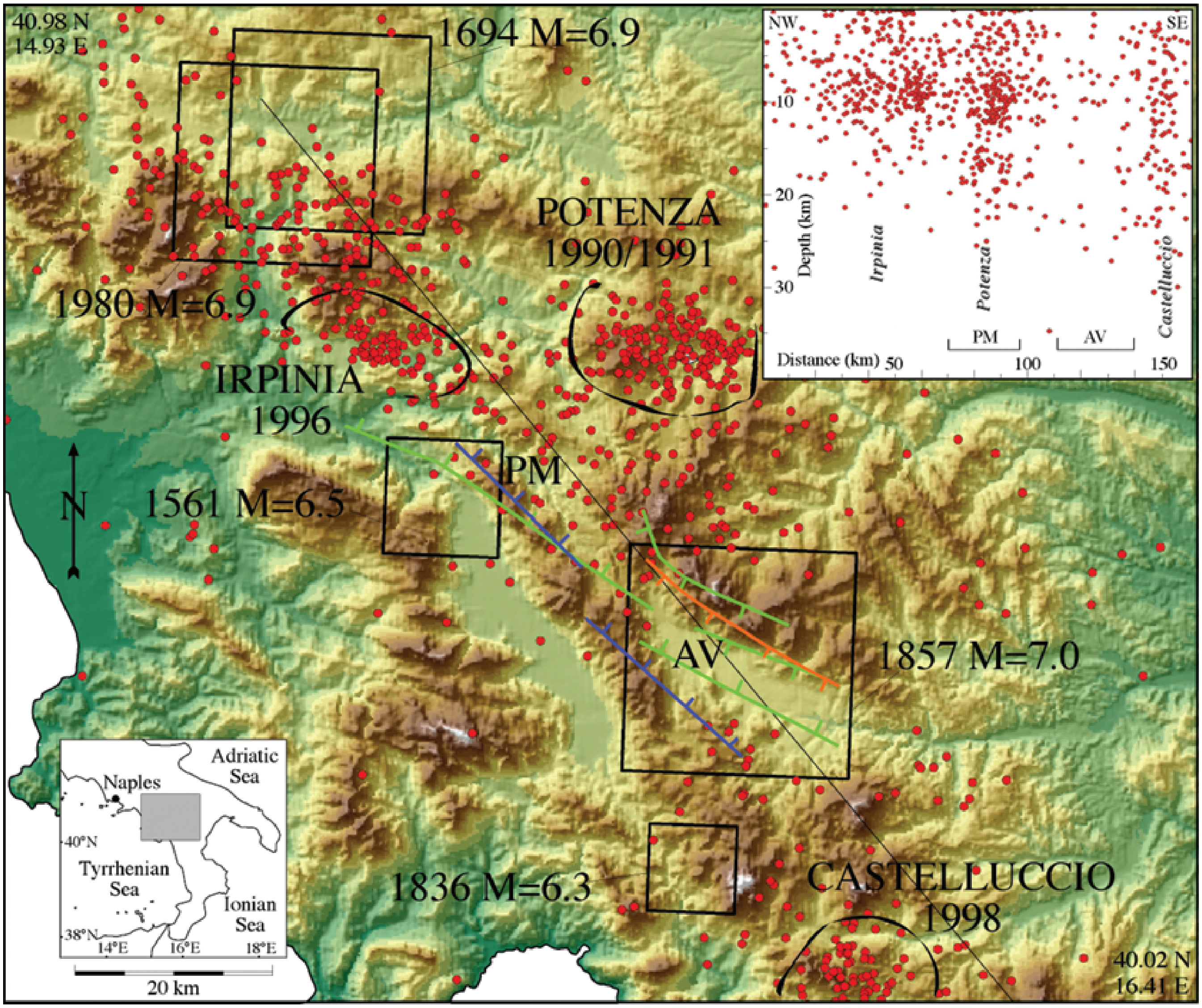

Figure 1. Historical and instrumental seismicity and tectonic features in and around the Pergola–Melandro Agri Valley region (PM and AV). $M > 6.0$ historical earthquakes (black squares) between 461 BC and AD 1997 are from Boschi *et al.* (2000). Instrumental seismicity (red dots) recorded in the period 1981–2000 by the RSNC (Italian Permanent Seismic Network) of the INGV and by the most important Italian local seismic networks (CSTI Working group, 1999). Most of the modern shocks are associated with the four sequences that occurred around the study area. The section in the upper right inset includes the projection of hypocenters located within a 90 km-wide strip along a *ca* 160 km-long, 50°NW direction (black thin line on map). Tectonic features in the study area are modified from Galadini *et al.* (2000) (green faults), Michetti *et al.* (2000) (brown faults) and Valensise & Pantosti (2001) (blue faults).

Potenza 1990 $Md = 5.5$ and 1991 $Ml = 5.2$, the 1996 Irpinia $Ml = 4.9$ and the 1998 Castelluccio $Md = 5.5$, all localized outside the study area; sparse seismicity affects the PM basin. The longitudinal 130°N-trending section (Fig. 1) across the map provides evidence of significantly broad zones almost completely devoid of seismicity in the central-northern AV; in particular, the major 1857 event is placed in this latter sector of instrumental gap. Therefore, AV was hit by a strong historical earthquake but lacks modern seismicity, and PM is marked by a slightly more diffuse microseismicity but with no historical event associated with it.

In this paper we present the results obtained following the production of new seismological and geophysical data and the revision of already existing data. To better constrain the direction pattern of the stress field we provide several new focal mechanisms determined either by waveform inversion or by *P*-wave first arrival polarities. We also study in detail two seismic sequences that occurred in 1996 and 2002 that are representative of the present-day activity. Further stress direction information is supplied by a number of breakout analyses. Together, all these data help to identify some characteristics of the seismotectonics in the study area such as the thickness of the seismogenic layer, the prevailing faulting mechanisms, the geometry of faults and the fit of local to regional stress field.

FOCAL MECHANISMS FROM WAVEFORM MODELLING AND *P*-WAVE POLARITIES

Focal mechanisms are one of the most important data used to understand the kinematics of an active tectonic area. The stress field information we can obtain from these kinds of data are a function of the magnitude of events.

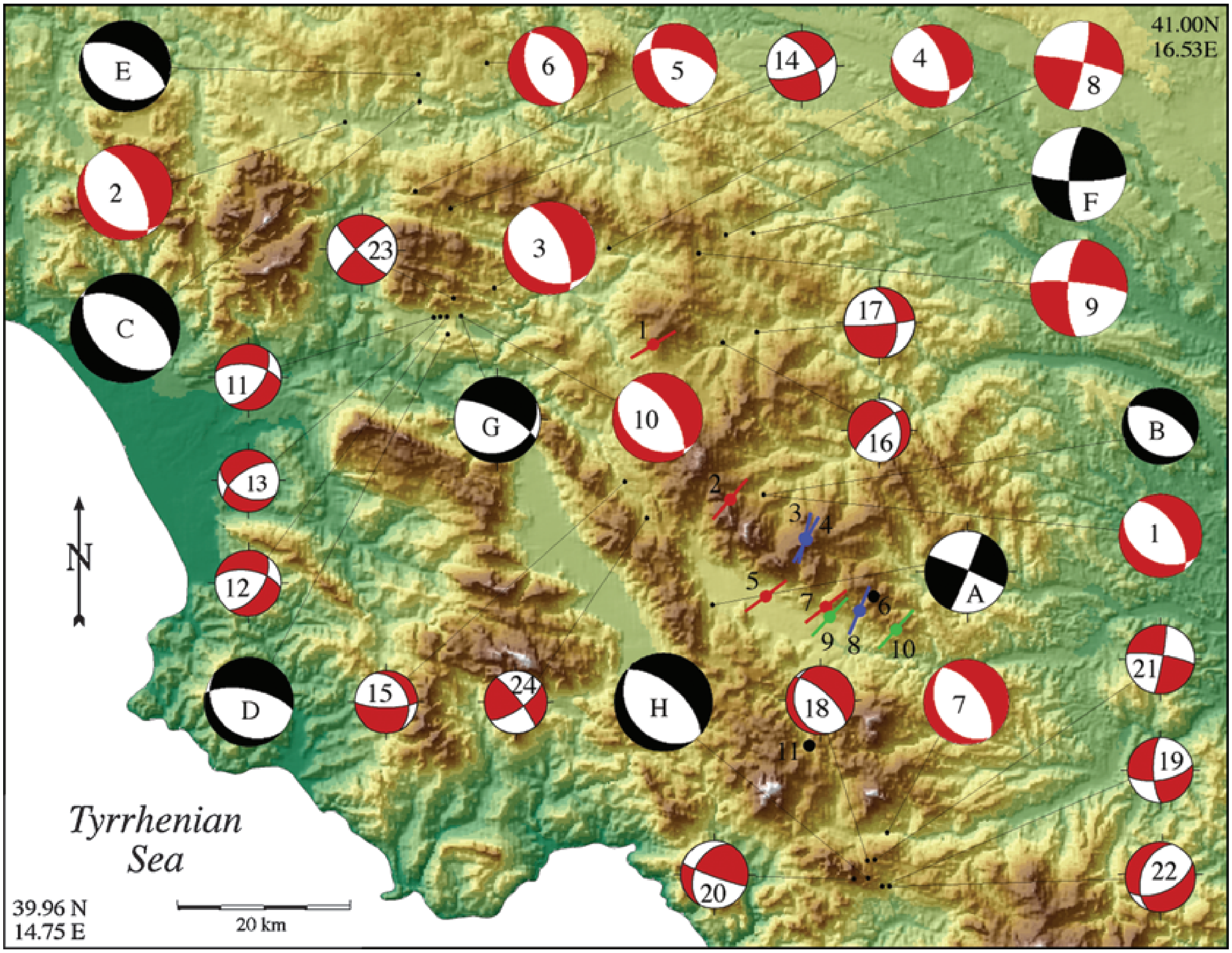

Figure 2. Focal plane solutions and breakout data in the study area. Black mechanisms are from the Harvard CMT Catalog, from Gasparini *et al.* (1985) and Cocco *et al.* (1999). Red mechanisms are from this work: n.1 to n.10 are from waveform inversion of $4.5 < M < 5.2$ earthquakes and n.11 to n.24 from *P*-wave first arrival polarities of $3.0 < M < 3.7$ earthquakes. Numbers and letters correspond to those of Table 1. Coloured bars indicate the minimum horizontal stress directions from borehole breakout analysis in deep oil wells with colours indicating decreasing well quality (Q): red = B, green = C, blue = D, black = E (discarded boreholes). Detailed information about each well are reported in Table 2.

For the study region, source parameters of some strong earthquakes are already available. In the Harvard CMT Catalog (quarterly reports in *Phys. Earth Planet. Int.,* see Dziewonski *et al.* 2001, and references therein) we discover the focal mechanisms of five events (Table 1 and Fig. 2, black focal mechanisms). The strongest event is the well known 1980 Irpinia earthquake (marked with C in Fig. 2 and Table 1), followed by two aftershocks (D and E in Fig. 2). The other two events are the $Mw = 5.7$, 1990 Potenza earthquake and the $Mw = 5.6$, 1998 Castelluccio earthquake (F and H in Fig. 2). Apart from the Harvard CMT Catalogue, the only focal mechanisms available are for two moderate magnitude events occurred within the study area in 1971 and 1980 (Gasparini *et al.* 1985, Table 1). In the European–Mediterranean RCMT Catalogue (Pondrelli *et al.* 2002) no solutions are present for the study area, showing that moderate seismicity was absent in the 1997–2001 period. Only recently, on 2002 April 18, a $Mw = 4.4$ earthquake occurred in the PM zone, starting a sequence that is discussed in the following paragraph.

Until the present work very few mechanisms of moderate magnitude events were available around the PM–AV area. Nonetheless, we found that the source parameters of a number of events were recoverable by waveform inversion because since 1997 a modification of the Harvard CMT method allows the computation of source parameters also for moderate magnitude events ($4.5 > M > 5.5$; Arvidsson & Ekström 1998). Instead of body waves, inverted in the standard CMT algorithm, surface waves are used, having the strongest amplitude at regional and teleseismic distance. This technique has already been extensively tested (Ekström *et al.* 1998; Pondrelli *et al.* 1999; Morelli *et al.* 2000) and is commonly used (Pondrelli *et al.* 2002). For 17 events with a magnitude greater than 4.5 (restricted to 5.0 only for the 1980 Irpinia seismic sequence) all available long period digital waveforms have been collected at IRIS. Thus, we obtained source parameters for only 10 of them (Table 1 and Fig. 2), since waveforms available were often of an insufficient quality to obtain a well constrained moment tensor solution. As expected none of the new solutions is within the PM–AV zone, but all of them are in agreement with the focal mechanism of strong earthquakes. The event n.1 in Table 1 is clearly extensional, as already found by Gasparini *et al.* (1985) using only polarities. The events n.2 and 3

Table 1. Source parameters: fault plane solutions of the study region. Numbers and letters correspond to those of Figure 2. Ref: wi, waveform inversions from this work; pol, solutions obtained by *P*-wave polarities in this work; HCMT, solutions from the Harvard CMT Catalogue (http://www.seismology.harvard.edu); Gas85, Gasparini *et al.* (1985); Cocco99, Cocco *et al.* (1999). Epicentral data and M_d magnitude for wi and HCMT data are from NEIS, for the others the magnitude is from INGV Bulletin and the coordinates are recomputed here. Borehole data.

N	Date	Time	Lat	Lon	Dep	M	Stri1	Dip1	Slip1	Stri2	Dip2	Slip2	M_0 (dyn*cm)	Ref.
A	71 11 29	18 49	40.34	15.77	4.0	4.7 M_d	203	86	−173	113	82	−4	—	Gas85
B	80 05 14	01 41	40.46	15.85	24	4.2 M_d	130	30	−79	120	69	−94	—	Gas85
1	80 05 14	01 41	40.46	15.85	24	4.5 M_b	119	38	−112	326	56	−74	2.23 e23	wi
C	80 11 23	18 34	40.91	15.37	10	6.9 M_s	135	41	−80	303	50	−98	2.47 e26	HCMT
2	80 11 24	00 24	40.89	15.26	10	5.1 M_L	131	29	−110	333	63	−79	4.52 e23	wi
3	80 11 25	17 06	40.70	15.47	10	5.1 M_L	122	30	−119	335	64	−74	3.11 e23	wi
D	80 11 25	18 28	40.65	15.40	10	5.3 M_s	129	26	−65	281	67	−102	1.51 e24	HCMT
E	81 01 16	00 37	40.94	15.37	15	5.3 M_s	115	30	−93	298	60	−89	8.47 e23	HCMT
4	81 11 29	05 06	40.74	15.64	15	4.9 M_L	104	41	−138	340	64	−58	7.28 e22	wi
5	82 08 15	15 09	40.81	15.36	10	4.8 M_L	158	48	−45	282	59	−128	1.20 e23	wi
6	87 01 28	05 33	40.95	15.47	10	4.6 M_L	160	45	−79	326	46	−100	8.16 e22	wi
7	88 01 08	13 05	40.08	16.01	10	4.8 M_b	148	30	−86	324	60	−92	1.41 e23	wi
F	90 05 05	07 21	40.75	15.85	26	5.6 M_d	184	73	13	90	78	162	5.67 e24	HCMT
8	90 05 05	07 38	40.75	15.81	15	5.0 M_d	282	83	173	13	83	7	2.06 e23	wi
9	91 05 26	12 26	40.73	15.77	8	5.2 M_L	183	71	−9	276	81	−160	5.25 e23	wi
10	96 04 03	13 04	40.67	15.42	10	4.9 M_d	111	15	−126	327	78	−81	2.80 e23	wi
G	96 04 03	13 04	40.67	15.42	10	4.9 M_d	64	25	−140	297	74	−70	—	Cocco99
11	96 07 16	12 46	40.67	15.38	12.2	3.4 M_d	45	45	−130	274	57	−57	—	pol
12	96 07 17	09 05	40.67	15.40	10.5	3.5 M_d	35	55	−140	279	58	−42	—	pol
13	96 08 22	06 47	40.67	15.39	10.0	3.0 M_d	115	45	−40	235	62	−127	—	pol
14	96 10 19	14 43	40.79	15.41	12.8	3.7 M_d	70	70	−150	328	61	−22	—	pol
15	97 07 15	10 49	40.48	15.65	7.0	3.1 M_d	90	75	−120	335	33	−28	—	pol
16	97 12 30	01 14	40.63	15.80	26.5	3.1 M_d	230	75	−60	344	33	−151	—	pol
17	98 04 26	05 38	40.64	15.85	13.8	3.7 M_d	85	85	−140	350	50	−6	—	pol
H	98 09 09	11 28	40.03	15.98	10	5.9 M_w	139	29	−83	311	61	−94	3.26 e24	HCMT
18	98 09 24	19 18	40.05	15.98	15.1	3.6 M_d	165	25	−60	312	68	−103	—	pol
19	98 09 25	00 44	40.02	16.00	13.8	3.3 M_d	80	65	−20	178	71	−153	—	pol
20	99 03 14	22 01	40.03	15.96	14.9	3.5 M_d	110	85	130	205	40	7	—	pol
21	99 04 05	04 16	40.05	15.99	10.1	3.6 M_d	10	85	−170	279	80	−5	—	pol
22	99 04 11	09 49	40.02	16.01	6.5	3.7 M_d	65	55	−60	199	44	−125	—	pol
23	99 07 21	13 56	40.69	15.41	15.4	3.3 M_d	135	80	−10	226	80	−169	—	pol
24	01 02 21	01 36	40.44	15.68	22.5	3.1 M_d	55	70	10	321	80	159	—	pol

are other aftershocks of the 1980 Irpinia seismic sequence and their focal mechanisms are in agreement with that of the main shock. The event n.8 is an aftershock of the 1990 Potenza earthquake. The event n.9, which occurred one year later, was previously unsolved because its body waves were perturbed by the waveforms of another teleseismic event (Ekström 1994); by using surface waves, we determined its source parameters. Both new solutions show a strike-slip geometry, in very close agreement with the 1990 main shock. The previously studied 1996 Irpinia earthquake, here with n.10, ruptured in the epicentral area of the 1980 Irpinia event (Cocco *et al.* 1999). Our focal solution has a slightly clockwise rotation compared to that (event G in Fig. 2) of Cocco *et al.* (1999), which was computed using *P*-wave polarities; however, this rotation may be related to the different determination methods. The other new solutions are for less known earthquakes. Most of them show an extensional geometry of rupture, confirming the tectonic trend of this area. Only a few events in the northeastern part of the study area show a strike-slip rupture.

In a seismotectonic framework where seismicity is scarce or often characterized by low magnitude, we also consider focal solutions to be significant for small events. We analysed *P*-wave first arrival polarities for 28 earthquakes with M_d ranging from 3.0 to 3.7 occurred in the region in the period 1996–2001 (previous seismicity and related focal mechanisms were already analysed in Frepoli & Amato 2000). A few events are concentrated in two small clusters. The first one is the previously mentioned 1996 Irpinia seismic sequence (main shock $Ml = 4.9$, Cocco *et al.* 1999), the second one is the September 1998 sequence of Castelluccio, close to the Basilicata–Calabria border (Fig. 1). All events show crustal hypocentral depths ranging between 6 and 26 km (mean error ±1.8 km). We obtained 14 fault plane solutions (Table 1) selected on the values of the quality factors Qf and Qp of the code FPFIT (Reasenberg & Oppenheimer 1985).

Therefore, the total amount of events for which new source parameters have been computed is 24 (Table 1, Fig. 2). T-axes of all moderate to large magnitude events show on average a NE–SW direction, also for strike-slip earthquakes of Potenza area. Decreasing the magnitude, T-axes prevailing orientations range between NE–SW and E–W. In the framework of the study region, these solutions agree significantly confirming the pre-dominance of the extensional regime affecting the southern Apennines.

ACTIVE STRESS FIELD FROM BOREHOLE BREAKOUT DATA

Several deep wells were drilled by ENI–AGIP SpA for oil exploration in the study area. Breakout analysis performed in some of them provided useful information about the active crustal stress in the region, especially regarding depths (from 500 m to about 6000 m)

Table 2. Details of the results of breakout analyses: well identification number, total depth reached by the borehole, range of the hole deviation from the vertical, analysed depth interval, breakout zone depth interval, minimum horizontal stress mean direction respect to the north, standard deviation, well quality. Digital data from the well studied in this paper were analysed using a software by Baker-Hughes.

Well	Depth (m)	Hole dev.	Anal. int. (m)	Break. int. (m)	Shmin	s.d.	Q
1	5760	1.5°–5°	5045–5390	5050–5377	59°	11°	B
2	4405	8°–18°	3356–4390	3753–4367	41°	12°	B
3	4390	0°–9°	200–4064	2307–3723	13°	33°	D
4	4722	10°–20°	3023–4722	3203–4161/4433–4602	29°	25°	D
5	3757	0.5°–3.5°	3017–3757	3037–3500	53°	11°	B
6	4400	0°–10°	1820–2726				E
7	3862	1°–3°	3138–3862	3153–3776	52°	11°	B
8	4090	2°–25°	1700–2993	1703–2109	23°	17°	D
9	4166	>10°	3163–4161	3670–3927	43°	22°	C
10	4910	0°–7°	4216–4882	4423–4638	42°	24°	C
11	4203	0°–11°	780–1965				E

between the surface and the seismogenic layer. We reviewed in detail all the available data from 10 wells previously analysed (Amato *et al.* 1995; Amato & Montone 1997; Mariucci *et al.* 2002) and analysed new data from one well (Fig. 2). A data quality rank was assigned to each well according to the World Stress Map Project (Zoback 1992), from A for the best quality to E for no reliable data. Detailed information about the breakout analysis are displayed in Table 2. Most of the breakout zones (five wells out of eleven) are located inside the carbonatic units of the Inner Apulian platform and in the terrigenous Lagonegro units (three wells). Although some boreholes were analysed from their top at shallow depths, the breakout zones are at depth, from 1700 m (well 8) to 5380 m (well 1), with prevailing data in the depth range between 3000 and 4500 m.

Nine wells out of eleven gave reliable mean Shmin directions: four B quality, two C, three D, and two wells were discarded E. Only in one case (well 3) the results with lower quality (D) show a main peak, in agreement with other breakout directions in the area, plus very scattered data in all directions; in the other wells (4 and 8) there are two preferential orientations, although they cannot be precisely attributed to different hole intervals. The two quality C results are characterized by two Shmin directions (well 9) and data scattering between a range from NNE to about ENE approximately (well 10). The best results (wells 1, 2, 5, 7), as can be deduced from the low standard deviation values, are formed by coherent and very close directions. Looking at the mean breakout directions in Fig. 2, the quality D data seem to show a Shmin direction slightly closer to *ca* NNE direction with respect to the other directions, clearly *ca* NE.

A detailed review of stratigraphic sequences drilled by the boreholes has been performed, to correlate the geological–structural setting and Shmin variations along depth. No defined intervals with breakout rotations, with respect to the general trend, possibly due to active faults crossing the borehole (as hypothesised by Mariucci *et al.* 2002), were found and no further analysis was possible.

Notwithstanding the different quality, all the data are coherent and indicate a mean Shmin direction *ca* NE–SW (range between 13°N and 59°N), even though data was obtained from different depths and the different structural units do not seem to influence the result. These Shmin directions agree with other active stress data in the southern Apennines, which define a tectonic regime in the area characterized by a general extension perpendicular to the belt (Amato *et al.* 1995; Amato & Montone 1997; Montone *et al.* 1999). In fact, the active stress horizontal directions found in this area are compatible with a normal fault tectonic regime with *ca* NW–SE oriented structures.

SEISMIC SEQUENCE IN THE STUDY AREA

We focused our attention on the two most significant seismic sequences that occurred in the study area during the last 20 yr. The first one, between 3 April and 12 June 1996, was localized along the southwestern side of the central AV (Fig. 3).The whole sequence has been completely reanalysed using arrival times at 27 different seismic stations that formed a network composed of: six stations from Italian permanent seismic network (RSNC); three from the Calabria regional seismic network (all equipped with vertical component short period seismometers); twelve digital three-component stations from the Istituto Nazionale di Geofisica e Vulcanologia (INGV) mobile network deployed during a monitoring experiment; and six digital three-component stations installed by INGV during the Geomodap teleseismic transect experiment (Amato *et al.* 1998). Most of the stations were located within 50 km of the shocks. In this study we used a 1-D velocity model derived by Amato & Selvaggi (1993) (Table 3) and the code HYPOELLIPSE (Lahr 1980) to locate the shocks. The events have formal location errors ranging between 0.5 and 2.0 km for the horizontal coordinates and between 1.0 and 2.5 km for the depth. The sequence data set numbers 50 low-magnitude events, with $1.8 \le Md \le 3.4$; the spatial distribution of seismicity during the sequence shows an Apenninic trend along a NW–SE direction, though most of the events are located within a distance of 5 km. The hypocentral distribution along a section perpendicular to the Apennines chain (Fig. 3) indicates that the shocks cluster at depth between 4 and 7 km. Although the distribution of the earthquakes does not allow to fully constrain the geometry of the fault plane at depth, the seismicity pattern on the SW–NE cross-section suggests the presence of a *ca* 50°NE dipping source. We analysed polarity data and determined focal mechanisms using FP-FIT code for the strongest events of this sequence (Fig. 3). 11 fault plane solutions out of 50 events showed good quality factors Qf and Qp. They are mostly normal fault solutions with a small strike-slip

Table 3. 1-D velocity model used to locate the shocks of the 1996 and 2002 sequences.

Vp (Km s^{-1})	H (Km)
4.5	0.0
5.7	6.0
6.5	10.0
8.1	30.0
$Vp/Vs = 1.81$	

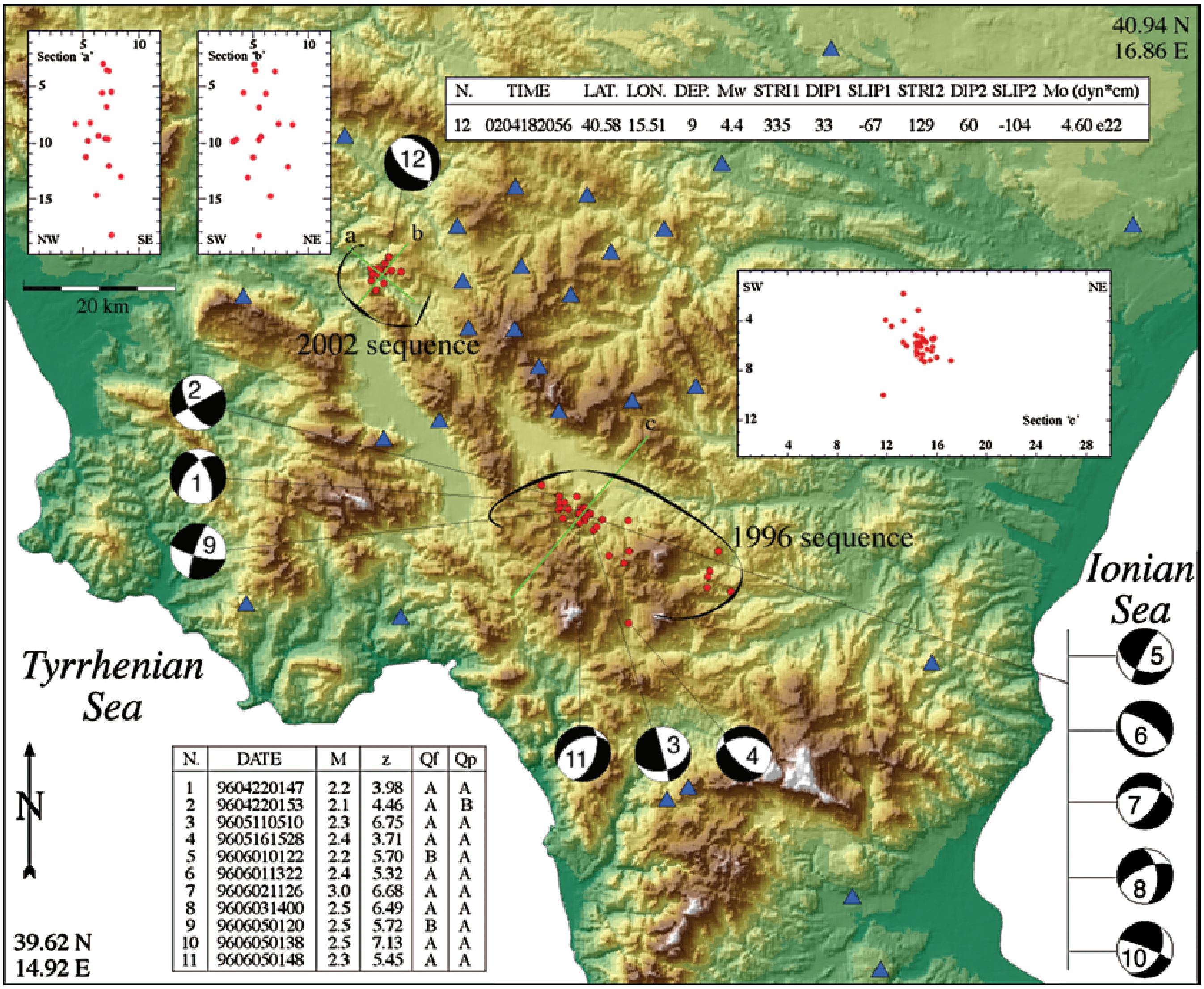

N.	TIME	LAT.	LON.	DEP.	Mw	STRI1	DIP1	SLIP1	STRI2	DIP2	SLIP2	Mo (dyn*cm)
12	0204182056	40.58	15.51	9	4.4	335	33	-67	129	60	-104	4.60 e22

N.	DATE	M	z	Qf	Qp
1	9604220147	2.2	3.98	A	A
2	9604220153	2.1	4.46	A	B
3	9605110510	2.3	6.75	A	A
4	9605161528	2.4	3.71	A	A
5	9606010122	2.2	5.70	B	A
6	9606011322	2.4	5.32	A	A
7	9606021126	3.0	6.68	A	A
8	9606031400	2.5	6.49	A	A
9	9606050120	2.5	5.72	B	A
10	9606050138	2.5	7.13	A	A
11	9606050148	2.3	5.45	A	A

Figure 3. The 1996 and 2002 seismic sequences. Red dots show earthquakes locations. Green lines (a, b, c) are cross-sections showing the hypocentral distribution. Focal mechanisms n.1 to n.11 belong to the 1996 sequence (parameters in the lower left table). Focal mechanism n.12 is the Quick Regional Moment Tensor solution (http://mednet.ingv.it/events/QRCMT/Welcome.html) of the 2002 main shock (source parameters in the upper right table; location errors: ERH = 1.2 km, ERZ = 0.9 km). Blue triangles indicate seismic stations used to locate the earthquakes.

component, although rather heterogeneous in the T-axis orientation. Only two are almost pure strike-slip focal mechanisms (Fig. 3, numbers 2 and 9). Nine of these solutions show T-axis oriented roughly NW–SE, while only two solutions (Fig. 3, number 4 and 6) show a T-axis orientated NE–SW.

Following a 20 yr-long period of scarce and spread microseismicity, on 2002 April 18, a second seismic sequence occurred along the northern side of the PM basin (Fig. 3). The seismicity distribution that we present here was obtained exclusively with data from RSNC. The $Mw = 4.4$ main shock occurred at a depth of 9 km, and was followed by a small number of $1.4 \leq \mathrm{Md} \leq 3.4$ aftershocks; the maximum location errors are 1.9 km both for the horizontal coordinates and for the depth except for four events with larger vertical error. The earthquakes distribution (Fig. 3) is rather concentrated within 3 km distance from the main shock. The hypocenters projected along two sections (parallel and perpendicular to the Apennines, respectively) show that the mean depths of the shocks range between 4 and 15 km and are, therefore, deeper than those of the 1996 sequence (Fig. 3). The limited number of hypocenters does not allow speculations about the dipping of the structure and, in any case, the Quick Regional CMT solution in Fig. 3 suggests a prevailing normal faulting mechanism with a *ca* NE–SW direction of extension for the main shock.

DISCUSSION

In this paper we reviewed all existing and recoverable seismological data and some geophysical data for the studied region. A general observation that can be made on the basis of these data is that the pattern of seismicity in the AV and PM areas is characterized by infrequent major strong events, like the 1561 and 1857 earthquakes, and by very low and sparse background seismic activity. In particular, there is no evidence of moderate magnitude ($5 \leq M \leq 6$) seismicity in the two study areas during the last 25 yr of instrumental catalogue, whilst $M + 5$ sequences, like the Irpinia 1980 and 1996, the Potenza 1990 and 1991, and the 1998 Castelluccio, occurred in the surrounding region. An analysis of focal mechanisms of major seismicity shows that most large and moderate magnitude

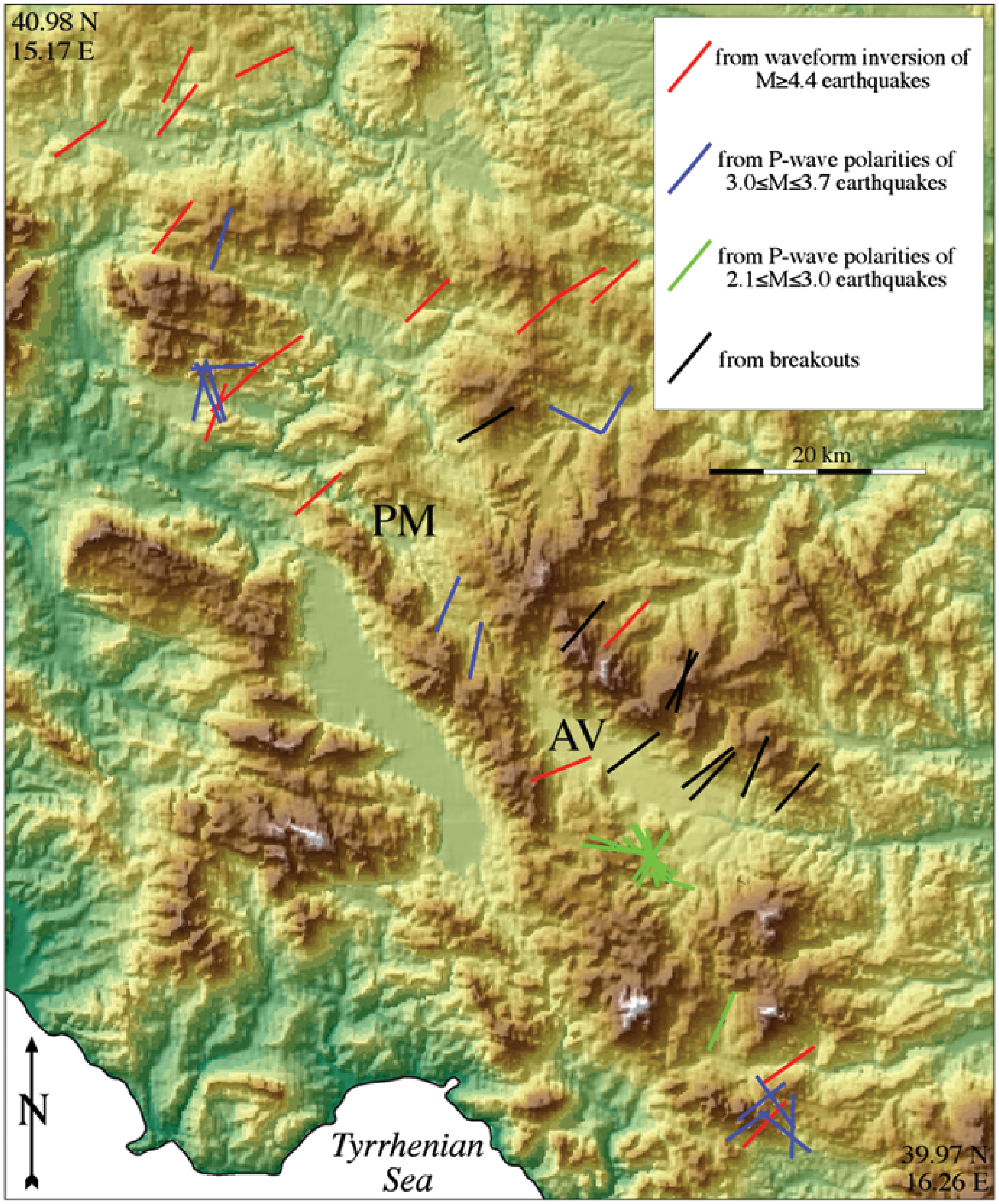

Figure 4. Summary map of all the collected data in terms of minimum horizontal stress orientations. Red bars are T-axes directions from CMT and RCMT ($4.4 \le M \le 6.9$), blue bars are T-axes directions from *P*-wave polarities focal mechanisms ($3.0 \le M \le 3.7$), green bars are T-axes directions from focal mechanisms of the 1996 sequence ($2.1 \le M \le 3.0$), and black bars are Shmin directions from breakout analyses. 37 directions out of 51 are original from this paper.

earthquakes are located between 5 and 15 km depth and display an extensional motion, with the T-axes usually NNE–ENE oriented. The 1990 and 1991 Potenza events are the only significant exception to this behaviour, with almost pure strike-slip mechanisms and greater hypocentral depths (e.g. 26 km for the 1990 event, Table 1; see also Azzara *et al.* 1993). However, these earthquakes also show NE–SW striking T-axes.

Focal mechanisms related to minor seismicity and to the two recent and most important sequences in the study area (southwestern AV and northern PM, respectively) confirm the tendency to an extensional regime, though with less homogeneity. Also, borehole breakout data are completely in agreement with the seismological data, displaying a persistent NE orientation of Shmin; in addition, breakout analyses allow consideration of activity of the extensional regime not only at seismogenic depth (from 5 to 15 km) but also toward the surface where this kind of technique samples the crust down to about 6 km. Figure 4 is a summary of all new data collected in this paper in terms of minimum horizontal stress directions, Shmin, in and around the study area. All the data (11 regional CMT of $4.4 \le M \le 5.2$ earthquakes, 25 other focal mechanisms of $2.1 \le M \le 3.7$ earthquakes, and 1 new plus 8 reviewed reliable Shmin directions from breakouts) delineate a seismotectonic pattern that is homogeneous in the area and consistent with that of the wider region of southern Italy. The extensional regime affecting since *ca* 0.7 Ma in most of the central-southern former Apennines thrust belt has already been described by several independent works (e.g. Ambrosetti *et al.* 1987; Pantosti *et al.* 1993; Westaway 1993; Hyppolite *et al.* 1994; Montone *et al.* 1999). The analysis of the data in Fig. 4 shows no significant short scale variations in stress orientation. Also, such strong homogeneity in the stress field pattern does not show any variations where it can be expected, such as along the NE–SW striking transversal structures that connect extensional basins within the chain. In the northern Apennines, moving eastward from the inner chain to its outer part, the stress regime changes from extensional to compressional (Frepoli & Amato 1997). Only a few tens of kilometers NW of the study area, in the Sannio–Matese region, studying a $Md = 4.1$ sequence Milano *et al.* (2004) found evidence of parallel, not perpendicular, extension along the Apennines seismogenic belt, with a stress regime locally consistent with normal movements along NE–SW faults. In the region studied here, these variations of orientation and/or type of stress are absent. These considerations support the hypothesis that earthquakes expected in the AV and PM areas would be mostly extensional, with extension in a NE–SW direction.

Although our data can not conclusively solve the controversy about the debated question of the dip of the main tectonic structures (Galadini *et al.* 2000; Michetti *et al.* 2000; Valensise & Pantosti 2001) there is a suggestion for a northeastward dipping along the PM and AV, mainly resulting from the observation of the denser seismicity distribution along the western sides of these two basins and from the hypocentral pattern (Figs 1 and 3). These observations are consistent with recent structural cross-sections based on seismic lines and deep wells (Menardi Noguera & Rea 2000), with the modelling of deformed recent geomorphological and geological features (Valensise & Pantosti 2001, Burrato and Valensise, in preparation) and with the damage distribution associated to the 1857 earthquake.

ACKNOWLEDGMENTS

This study was supported by the GNDT Project, '*Probable earthquakes in Italy from year 2000 to 2030: guidelines for determining priorities in seismic risk mitigation*', coordinated by A. Amato. Thanks are due to all contributors of Task 1.4, '*Characterization of the seismogenic sources in areas of seismic gap*', lead by P. Montone. L.C. wants to thank L. Margheriti, M. Cattaneo, M. Demartin and S. Pierdominici of INGV and A. Gervasi of the University of Calabria for helping with seismological and geological data retrieval. S.P. thanks A. Morelli and G. Ekström for the availability of RCMT computation codes and for invaluable assistance with the moment tensor study. A.F. thanks P. De Gori for helping in the realization of some focal mechanisms. M.T.M. thanks M. Cesaro of ENI-AGIP. Valuable discussions, important suggestions and comments arose from the examination of an early draft of the paper by P. Gasperini, P. Montone and F.R. Cinti. Special thanks to the Editor R. Madariaga for a thorough review and kind availability. The IRIS seismological data have been downloaded from: http://www.iris.washington.edu.

REFERENCES

Amato, A.*et al*., 1998. Passive seismology and deep structure in Central Italy, *Pure appl. Geophys.*, **151,** 479–493.

Amato, A., Montone, P. & Cesaro, M., 1995. State of stress in Southern Italy from borehole breakout and focal mechanism data, *Geophys. Res. Lett.*, **22,** 3119–3122.

Amato, A. & Montone, P., 1997. Present-day stress field and active tectonics in southern peninsular Italy, *Geophys. J. Int.*, **130,** 519–534.

Amato, A. & Selvaggi, G., 1993. Aftershock location and P-velocity structure in the epicentral region of the 1980 Irpinia earthquake, *Annali di Geofisica,* **36,** 3–25.

Ambrosetti, P., Bosi, C., Carraro, F., Ciaranfi, N., Panizza, M., Papani, G., Vezzani, L. & Zanferrari, A., 1987. Neotectonic Map of Italy, *Quad. Ric. Scient.,* **114,** 4.

Arvidsson, R. & Ekström, G., 1998. Global CMT Analysis of Moderate Earthquakes $Mw > 4.5$ using Intermediate Period Surface Waves, *Bull. seism. Soc. Am.,* **88,** 1003–1013.

Azzara, R., Basili, A., Beranzoli, L., Chiarabba, C., Di Giovambattista, R. & Selvaggi, G., 1993. The seismic sequence of Potenza (May 1990), *Ann. Geofis.,* **36,** 237–243.

Boschi, E., Guidoboni, E., Ferrari, G., Mariotti, D., Valensise, G. & Gasperini, P., 2000. Catalogue of Strong Italian Earthquakes, *Ann. Geofis.,* **43,** 4, 609–868.

Cinti, F.R., Cucci, L., Pantosti, D., D'Addezio, G. & Meghraoui, M., 1997. A major seismogenic fault in a 'silent area': the Castrovillari fault (southern Apennines, Italy), *Geophys. J. Int.,* **130,** 322–332.

Cinti, F.R., Moro, M., Pantosti, D., Cucci, L. & D'Addezio, G., 2002. New constraints on the seismic history of the Castrovillari fault in the Pollino gap (Calabria, southern Italy), *J. Seism.,* **6,** 199–217.

Cocco, M.*et al*., 1999. The April 1996 Irpinia seismic sequence: Evidence for fault interaction, *J. Seism.,* **3,** 105–117.

CSTI Working group, 1999. *Catalogo strumentale dei terremoti italiani dal 1981 al 1996. Database on CD-ROM*, *INGV-GNDT*. Also available at: http://ibogfs.df.unibo.it/user2/paolo/www/gndt.html.

Dziewonski, A.M., Ekström, G. & Maternovskaya, N.N., 2001. Centroid-moment tensor solutions for April–June 2000, *Phys. Earth Planet. Int.,* **123,** 1–14. Also at: http://www.seismology.harvard.edu.

Ekström, G., 1994. Teleseismic analysis of the 1990 and 1991 earthquakes near Potenza, *Ann. Geofis.,* **37,** 1591–1599.

Ekström, G., Morelli, A., Boschi, E. & Dziewonski, A.M., 1998. Moment tensor analysis of the central Italy earthquake sequence of September–October 1997, *Geophys. Res. Lett.,* **25,** 1971–1974.

Frepoli, A. & Amato, A., 1997. Contemporaneous extension and compression in the Northern Apennines from earthquake fault plane solutions, *Geophys. J. Int.,* **129,** 368–388.

Frepoli, A. & Amato, A., 2000. Fault plane solutions of crustal earthquakes in Southern Italy (1988–1995): seismotectonic implications, *Ann. Geofis.,* **43,** N.3, 437–467.

Galadini, F., Meletti, C. & Vittori, E., 2000. Stato delle conoscenze sulle faglie attive in Italia: elementi geologici di superficie, in *Le ricerche del GNDT nel campo della pericolositá sismica (1996–1999)*, pp. 1–397, eds Galadini F., Melett, C. & Rebez, A., Internal report of CNR-Gruppo Nazionale per la Difesa dai Terremoti, Roma.

Gasparini, C., Iannaccone, G. & Scarpa, R., 1985. Fault-plane solutions and seismicity of the Italian peninsula, *Tectonophysics,* **117,** 59–78.

Hyppolite, J.-C., Angelier, J. & Roure, F., 1994. A major geodynamic change revealed by Quaternary stress patterns in the Southern Apennines (Italy), *Tectonophysics,* **230,** 199–210.

Lahr, J.C., 1980. *HYPOELLIPSE/MULTICS: a computer programme for determining local earthquake hypocentral parameters, magnitude, and first motion pattern,* p. 59, U.S. Geological Survey Open-File Report 80–59.

Mariucci, M.T., Amato, A., Gambini, R., Giorgioni, M. & Montone, P., 2002. Along-depth stress rotations and active faults: an example in a 5-km deep well of Southern Italy, *Tectonics,* **21,** 1–9.

Menardi Noguera, A. & Rea, G., 2000. Deep structure of the Campanian-Lucanian Arc (Southern Apennine, Italy), *Tectonophysics,* **324,** 239–265.

Michetti, A.M., Ferreli, L., Serva, L. & Vittori, E., 1997. Geological evidence for strong historical earthquakes in an 'aseismic' region: the Pollino case (southern Italy), *J. Geodyn.,* **24,** 67–86.

Michetti, A.M., Serva, L. & Vittori, E., 2000. *ITHACA (Italy hazard from Capable Faulting), a database of active capable faults of the Italian onshore territory. Database on CD-ROM,* Internal report of ANPA-Agenzia Nazionale Protezione Ambiente, Roma.

Milano, G., Ventura, G. & Di Giovambattista, R., 2004. Seismic evidence of longitudinal extension in the Southern Apennines chain (Italy): The 1997–1998 Sannio-Matese seismic sequence, *Geophys. Res. Lett.,* **29(20),** doi:10.1029/2002GL015188, 2002.

Montone, P., Amato, A. & Pondrelli, S., 1999. Active stress map of Italy, *J. geophys. Res.,* **104,** 25 595–25 610.

Morelli, A., Ekström, G. & Olivieri, M., 2000. Source properties of the 1997–98 Central Italy earthquake sequence from inversion of long-period and broad-band seismograms, *J. Seism.,* **4,** 365–375.

Omori, F., 1909. Preliminary report on the Messina-Reggio Earthquake of Dec. 28, 1908, *Bull. Imperial Earthquake Invest. Comm.,* **3–2,** 37–46.

Pantosti, D., Schwartz, D.P. & Valensise, G., 1993. Paleoseismology along the 1980 surface rupture of the Irpinia fault: implications for earthquake recurrence in the southern Apennines, Italy, *J. geophys. Res.,* **96,** 6561–6577.

Pantosti, D., D'Addezio, G. & Cinti, F.R., 1996. Paleoseismicity of the Ovindoli-Pezza fault (Central Italy): a history including a large, previously unrecorded earthquake in Middle Ages (860–1300 A.D.), *J. geophys. Res.,* **101,** 5937–5959.

Pondrelli, S., Ekström, G., Morelli, A. & Primerano, S., 1999. Study of source geometry for tsunamigenic events of the Euro-Mediterranean area, in *International Conference on Tsunamis*, pp. 297–307, ed. Massinon, B., UNESCO books, Paris.

Pondrelli, S., Morelli, A., Ekström, G., Mazza, S., Boschi, E. Dziewonski, A.M., 2002. European-Mediterranean regional centroid-moment tensors: 1997–2000, *Phys. Earth planet. Int.,* **130,** 71–101. (Quick Regional CMT available at: http://mednet.ingv.it/events/QRCMT/Welcome.html)

Reasenberg, P. & Oppenheimer, D., 1985. FPFIT, FPPLOT and FPPAGE: FORTRAN computer programs for calculating and displaying earthquake fault-plane solutions, in, *U.S. Geol. Surv. Open-File Rep.,* pp. 85–739, U.S. Geol. Surv.

Valensise, G. & Pantosti, D., 2001. eds. Database of potential sources for earthquakes larger than M 5.5 in Italy, *Suppl. to Ann. Geofis.,* **44**, 4, 797–964.

Valensise, G., Pantosti, D., D'Addezio, G., Cinti, F.R. & Cucci, L., 1993. L'identificazione e la caratterizzazione di faglie sismogenetiche nell'Appennino centro-meridionale e nell'arco calabro: nuovi risultati e ipotesi interpretative, *Atti XII Convegno G.N.G.T.S.*, *Roma,* 331–342.

Westaway, R., 1993. Quaternary uplift of Southern Italy, *J. geophys. Res.,* **98,** 21 741–21 772.

Zoback, M.L., 1992. First and second order patterns of stress in the lithosphere: the World Stress Map Project, *J. geophys. Res.,* **97,** 11 703–11 728.